# Binary Asteroid Population. 1. Angular Momentum Content

P. Pravec [a], A.W. Harris [b],

[a] *Astronomical Institute, Academy of Sciences of the Czech Republic, Fričova 1, CZ-25165 Ondřejov, Czech Republic*

[b] *Space Science Institute, 4603 Orange Knoll Ave., La Canada, CA 91011, USA*

Version: 2006 Nov. 15, submitted

Proposed running head: Angular momentum in binary asteroids

Editorial correspondence to:
Dr. Petr Pravec
Astronomical Institute AS CR
Fričova 1
Ondřejov
CZ-25165
Czech Republic
Phone: 00420-323-620352
Fax: 00420-323-620263
E-mail address: ppravec@asu.cas.cz

**Abstract**

We compiled a list of estimated parameters of binary systems among asteroids from near-Earth to Trojan orbits. In this paper, we describe the construction of the list, and we present results of our study of angular momentum content in binary asteroids. The most abundant binary population is that of close binary systems among near-Earth, Mars-crossing, and main belt asteroids that have a $D_p$ of about 10 km or smaller. They have a total angular momentum very close to, but not generally exceeding, the critical limit for a single body in a gravity regime. This suggests that they formed from parent bodies spinning at the critical rate (at the gravity spin limit for asteroids in the size range) by some sort of fission or mass shedding. The candidate cause of spin-up to instability is the Yarkovsky-O'Keefe-Radzievskii-Paddack (YORP) effect. Gravitational interactions during close approaches to the terrestrial planets cannot be a primary mechanism of formation of the binaries, but it may affect properties of the NEA part of the binary population.

*Key words:* Asteroids, binary;

## 1 Introduction

A wealth of data on binary asteroid systems has been obtained over the past several years. We now have a few times more data on binaries than existed at the time of the summary by Merline et al. (2002) in *Asteroids III*. The quality of the data has increased since that time as well. We were interested in what the rapidly growing data on the properties of the binary population could tell us, especially among the small asteroids. Therefore, we compiled data on binaries from NEA to Trojan orbits. In this paper, we introduce the data set and the results from our initial studies concerning the angular momentum content in binary asteroids. We then use the data to discuss proposed formation mechanisms.

## 2 Data set

We have compiled estimated parameters for 73 binary systems in near Earth, Mars crossing, main belt, and Trojan orbits. The dataset is available on web page http://www.asu.cas.cz/∼asteroid/binastdata.htm. References to the data are given in file on the web page as well as in the References section of this paper.

We were careful to give realistic uncertainties for the compiled estimates. Published formal errors of the estimated parameters are normally given. In some cases, where no uncertainty has been published for a particular estimated parameter or where we have a reason to believe that an actual uncertainty may be greater (e.g., because authors did not account for some additional significant source of uncertainty in the given parameter estimate), we have either attempted to estimate the uncertainty ourselves (sometimes following a discussion with the authors), or we assigned some typical uncertainty for the given parameter estimated with the given technique.

For derived quantities, we propagated uncertainties of actually measured quantities (or assumed ranges for some) so that the derived quantity is always given with an uncertainty that is immediately related to the measured ones.

### *2.1 Measured and directly estimated quantities*

#### *$D_p$, $D_s$, and the size ratio $X$*

Absolute sizes of the components are parametrized with their mean diameters at the equatorial aspect, denoted by $D_p$ and $D_s$, while the relative size of the components is parametrized with a ratio of the two diameters, $X \equiv D_s/D_p$. The reason for this choice of parameters is that asteroid size determination methods mostly estimate cross-section (rather than, e.g., volume). So, a mean

diameter corresponding to cross-section ($S \equiv \pi D^2/4$) is a size parameter that is directly related to measurements in most cases. The choice of the equatorial aspect is because the most straightforward estimate of the ratio of mean diameters (i.e., cross-sections) of the components of a binary system is made from photometric observations of total mutual events that occur at nearly equatorial aspects. From works where other size parameters have been estimated, we converted them to $D_p$ and $D_s$. For example, where the semimajor axes $(a_1, b_1, c_1)$ of an ellipsoid approximating the primary have been given, we converted them to $D_p$ using following formula

$$D_p = \sqrt{2(a_1 + b_1)c_1} \tag{1}$$

obtained from a mean cross-section of the ellipsoid at the equatorial aspect.

Obviously, only two of the three parameters –$D_p, D_s$, and $X$– had to be estimated from the observations; the remaining one was derived from the other two.

*$H$ and $p_V$*

Where the absolute sizes were not estimated directly, we derived them from an absolute magnitude and a geometric albedo. In a number of cases, the absolute magnitude at the equatorial aspect in the Johnson $V$ band ($H$) had been estimated from photometric observations.[1] In some cases where no accurate absolute photometry was available, we used rough $H$ estimates obtained by the *Minor Planet Center* from astrometric data; an uncertainty of $\pm 0.5$ was assigned to each such value since the astrometric $H$ estimates showed that much scatter when compared to accurate photometric $H$ values. The geometric albedo on the Johnson $V$ band ($p_V$) had to be assumed in a number of cases. When an estimated spectral type or a family membership assignment was available, the geometric albedo could be constrained accordingly. In the remaining cases, we assumed $p_V = 0.18 \pm 0.09$ that is appropriate for S type asteroids that prevail observationally among the NEAs, Mars-crossers, and inner main belt asteroids.

The relation between $H$, $p_V$, $D_p$ and $D_s$ (assuming the same albedo for both components[2]) is

$$D\sqrt{p_V} = K \cdot 10^{-H/5}, \tag{2}$$

[1] In cases where the absolute magnitude $H_R$ in the Cousins $R$ system was estimated, it was converted to $H \equiv H_V$ using a $V-R$ value that was either measured, or derived (e.g., from spectral observations), or assumed.

[2] Data on well observed binaries are consistent with the same albedo assumption.

where $K = 1329$ km (see Appendix[3]), and the effective diameter is

$$D \equiv \sqrt{D_p^2 + D_s^2} = D_p\sqrt{1 + X^2}. \quad (3)$$

In cases where only the size ratio had been estimated, $D_p$ and $D_s$ were derived from $H$ and $p_V$ using Eqs. 2 and 3.

*$P_{prim}$ and $P_{sec}$*

Primary and secondary rotation periods were estimated from lightcurve or radar data. In cases where there was only an estimated synodic rotation period and its synodic-sidereal difference (Eq. 8 in Pravec et al., 2005) was estimated to be greater than the formal uncertainty of the estimated synodic period, we adopted the synodic-sidereal difference as the period uncertainty in our dataset so that it represented a sidereal period.

*$P_{orb}$*

Orbital periods were estimated through orbital fits to astrometric or radar data or from the recurrence of mutual events in photometrically detected binaries. As in the case of rotation periods, adopted uncertainties account for synodic-sidereal effects so that the estimates with the given error bars represent sidereal periods.

*$A_{prim}$ and $A_{sec}$*

Amplitudes of the lightcurve components were compiled in cases where there were no modeled $a/b$ estimates available. Since the amplitudes were obtained at mostly near-equatorial aspects (during seasons of mutual events), they could be used for an approximate estimation of the equatorial elongation of the bodies. The ratio of maximum and minimum cross-sections is estimated by

$$B = 10^{0.4A_0}, \quad (4)$$

where the amplitude at zero solar phase is estimated using the empiric linear correction for the amplitude-phase effect by Zappalà et al. (1990):

$$A_0 = \frac{A}{1 + m\alpha}, \quad (5)$$

where we assumed $m/1^\circ = 0.02 \pm 0.01$, and $\alpha$ is a reference angle at which the amplitude ($A_{prim}$, $A_{sec}$) was measured.

[3] The relation among $D, H$, and $p_V$ has not been given in the literature (other than "grey") for long time. We give its derivation and discuss it further in the Appendix.

Since the observed amplitude is always affected (lowered) by the presence of light from the other component,[4] a correction of the amplitude for the estimated size ratio ($X \equiv D_s/D_p$) must be included in the estimate for $a/b$.

*$a/b_{prim}, b/c_{prim}, a/b_{sec}, b/c_{sec}$*

Estimated ratios of ellipsoids approximating the components were compiled. Where there was a non-ellipsoidal shape estimated for a given body and ratios of its principal moments of inertia given, we compiled axial ratios of a dynamically equivalent ellipsoid (i.e., an ellipsoid with the same moments of inertia). Where there was no estimate of an axial ratio available, we assumed for purposes of derivation of the other parameters the following ratios: Primary's default axial ratios: $a/b_{prim} = b/c_{prim} = 1.1 \pm 0.1$. Secondary's default axial ratios: $a/b_{sec} = b/c_{sec} = 1.3 \pm 0.2$ for $X < 0.85$, and $a/b_{sec} = b/c_{sec} = 1.1 \pm 0.1$ for $0.85 \leq X \leq 1$.

*Orbital semimajor axis $A$ and $A/D_p$*

We denote the orbital semi-major axis with the capital letter ($A$) throughout this paper to avoid confusion with the largest semi-axis $a$ of a body. In some cases, the orbital semi-major axis was estimated directly from orbital fits to observational data. In other cases, however, only the ratio of $A/D_p$ was estimated through modeling, or it was derived from estimated values for $P_{orb}$, $D_p$, and $X$ using Kepler's Third Law. (Some other unconstrained quantities, e.g., bulk density, had to be assumed with plausible ranges in such cases; see below).

*Bulk density $\rho$*

We derived the bulk density with Kepler's Third Law in cases where $A, P_{orb}$, $D_p$, and $D_s$ were estimated from observational data. The largest uncertainty in derived $\rho$ values usually arose from poorly known volume of the body; since $V \sim D_p^3$, a 10% uncertainty in size propagates to a 30% uncertainty in $\rho$. Moreover, actual shapes may be irregular, which further increases the ratio between the cross-section and the volume of a body. We remind that most methods of size estimation actually measure the cross-section rather than the volume and so there is a systematic source of error towards overestimating the volume, hence underestimating the bulk density.

Where the bulk density could not be estimated, we assumed it to be 2.0 g/cm$^3$ with an uncertainty factor of 1.5. We assumed that it encompasses at least 2/3 of observed binary systems.

[4] Amplitudes reduced to a mean light level of the other component is given; see Pravec et al. (2006).

### *2.2 Other used quantities*

*Mass ratio q*

Throughout this paper, we assume that both components have the same density. The mass ratio $q \equiv M_2/M_1$ can be estimated as

$$q = X^3 \left\{ \left[ \frac{\left(\frac{a_1}{b_1}+1\right)\frac{b_2}{c_2}}{\left(\frac{a_2}{b_2}+1\right)\frac{b_1}{c_1}} \right]^{\frac{3}{2}} \frac{\frac{a_2}{b_2}\frac{b_1}{c_1}}{\frac{a_1}{b_1}\frac{b_2}{c_2}} \right\} \tag{6}$$

The term in brackets accounts for different shapes of the components; for components with $a_1/b_1 = a_2/b_2$ and $b_1/c_1 = b_2/c_2$, the term in brackets is equal to 1 and the mass ratio is simply the third power of the ratio of the mean diameters at equatorial aspect.

### *2.3 "Factor of" uncertainties*

For most derived quantities as well as for some measured or assumed ones, we give the uncertainty in the form of "a factor of". This is actually equivalent to a "±" uncertainty of the logarithm of the quantity. Formally, it can be written as

$$X \text{ uncertain by factor f}X \;\Leftrightarrow\; Y \pm \delta Y, \tag{7}$$

where

$$Y \equiv \log X, \quad \delta Y \equiv \log \mathrm{f}X.$$

For some purposes, an approximate conversion of f$X$ to a "±" error $\delta X$ that is valid for $(\mathrm{f}X - 1) \ll 1$ is

$$\frac{\delta X}{X} \doteq \mathrm{f}X - 1. \tag{8}$$

## 3 Angular momentum in binary asteroids

The total angular momentum $\vec{L}$ in a binary asteroid can be given as

$$\vec{L} = \vec{L}_1 + \vec{L}_2 + \vec{L}_{orb}, \tag{9}$$

where $\vec{L}_i$ is the rotational angular momentum of the $i$-th body (1 for primary, 2 for secondary), and $\vec{L}_{orb}$ is the orbital angular momentum. Assuming that both components are in their basic states of rotation around their principal axes with the maximum moments of inertia ($I_i$), then their rotational angular momenta are

$$\vec{L}_i = I_i \vec{\omega}_i, \tag{10}$$

where $\vec{\omega}_i$ is the angular velocity vector of the $i$-th body. The orbital angular momentum is

$$\vec{L}_{orb} = \frac{M_1 M_2}{M_1 + M_2} A^2 (1 - e^2)^{1/2} \vec{n}, \tag{11}$$

where $M_i$ is the mass of the $i$-th body, $A$ is the semimajor axis, $e$ is the orbital eccentricity, and $\vec{n}$ is the orbital rate.

In the following, we will assume that all the vectors mentioned above are parallel, hence the magnitude of the total angular momentum vector is the sum of the magnitudes of the two rotational angular momentum vectors and the orbital angular momentum vector. In a general case of non-parallel vectors, the sum of the vector magnitudes is an upper limit on the magnitude of the total angular momentum vector. Observations and theoretical considerations [5] suggest that most binary asteroids are close enough to the assumed state so that the approximate estimation of the magnitude of the total angular momentum as a sum of magnitudes of the individual momentum vectors is good enough for our purposes.

It will be convenient to have the angular momenta expressed using the mass ratio $q \equiv M_2/M_1$ and the total mass of the system $M \equiv M_1 + M_2$:

$$L_1 = \frac{M}{5(1+q)} (a_1^2 + b_1^2) \omega_1, \tag{12}$$

$$L_2 = \frac{qM}{5(1+q)} (a_2^2 + b_2^2) \omega_2, \tag{13}$$

[5] Periods of nodal precession of satellite orbit for the closest systems with $P_{orb} \approx$ 14 h are less than 100 days for primary's $J_2 > 0.05$ (a moderate flattening), so if the inclination of the satellite orbit was greater than $\approx 10^\circ$, a characteristic evolution of observed mutual events would be seen in a few weeks of observations. Such evolution is not observed.

$$L_{orb} = \frac{qM}{(1+q)^2} A^2 n (1-e^2)^{1/2} =$$

$$= \frac{qM}{(1+q)^{4/3}} (V_1 \rho G)^{2/3} n^{-1/3} (1-e^2)^{1/2}, \tag{14}$$

where $a_i, b_i, c_i$ are semiaxes of the dynamically equivalent equal mass ellipsoid (DEEME) of the $i$-th body, and $V_1$ is the volume of the primary. We remind that the bulk density $\rho$ is assumed to be the same for both components.

A quantity that interests us is the ratio between the total angular momentum of the system and the angular momentum of a critically spinning equivalent sphere (i.e., a sphere of the same total mass and volume as the two components of the binary system) with the angle of friction $\phi = 90^\circ$ (cf. Sect. 3.2). We denote the ratio $\alpha_L$.

The angular momentum of the equivalent sphere spinning at the critical spin rate is

$$L_{eqsph} = \frac{2}{5} M \left( \frac{3}{4\pi} V_1 \right)^{2/3} (1+q)^{2/3} \omega_{csph}, \tag{15}$$

where $\omega_{csph}$ is the critical spin rate for the sphere with $\phi = 90^\circ$ and density $\rho$

$$\omega_{csph} = \sqrt{\frac{4}{3}\pi\rho G}, \tag{16}$$

where G is the gravitational constant.

The ratio $\alpha_L$ (normalized total angular momentum of the binary system) is then expressed as

$$\alpha_L \equiv \frac{L_1 + L_2 + L_{orb}}{L_{eqsph}} =$$

$$= \frac{\left[1 + \left(\frac{a_1}{b_1}\right)^2\right] \omega_1 + q \left(\frac{b_2}{b_1}\right)^2 \left[1 + \left(\frac{a_2}{b_2}\right)^2\right] \omega_2}{2(1+q)^{5/3} (\nu \frac{a_1}{b_1} \frac{c_1}{b_1})^{2/3} \omega_{csph}} +$$

$$+ \frac{5}{2} \frac{q}{(1+q)^2} \left( \frac{\omega_{csph}}{n} \right)^{\frac{1}{3}} (1-e^2)^{1/2}, \tag{17}$$

where $\nu \equiv V_1 / V_{DEEME1} = V_1 / (a_1 b_1 c_1 \pi 4/3)$ is the ratio between the volume of the primary and the volume of the dynamically equivalent equal mass ellipsoid of the primary.

Eq. 17 contains parameters that have been mostly well estimated ($\omega_1, n$), or such for which reasonable estimates or assumptions [6] could be made and their propagated uncertainties do not cause a large uncertainty in $\alpha_L$. Resulting uncertainties in $\alpha_L$ are typically 10 to 20%, and less than 30% in all cases where $\alpha_L$ could be computed.

One parameter that was not estimated is the ratio $\nu$ between the volume of the primary and the volume of the dynamically equivalent equal mass ellipsoid of the primary. We assumed it to be equal to 1. A current poor knowledge of real shapes of the primaries does not allow us to place a meaningful uncertainty range to the assumed $\nu = 1$, but it seems that most primaries have reasonably regular shapes and we think that the assumption of $\nu = 1$ does not cause an error in $\alpha_L$ greater than the resulting propagated uncertainties from the other parameters mentioned above.

[6] Eccentricities have not been estimated precisely for most binaries, but they appear nearly zero in most cases. Since the eccentricity in Eq. 17 affects the result by a factor of $(1 - e^2)^{1/2}$, an error in $\alpha_L$ caused by assuming zero eccentricity is less than 1 and 5% for $e < 0.1$ and 0.3, respectively; we went with the zero eccentricity assumption.

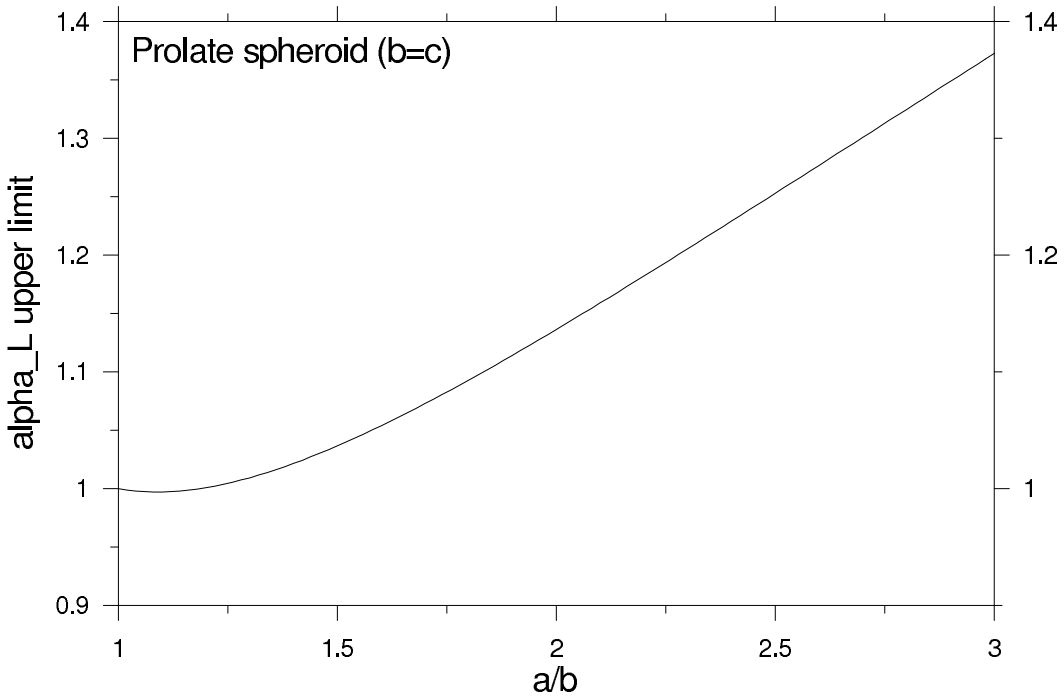


Fig. 1. An upper limit on $\alpha_L$ for a prolate strengthless spheroid with the angle of friction of 90° vs. $a/b$. For asteroids in gravity regime (i.e., with zero or low tensile strength) with plausible angles of friction ($\approx 40°$), the upper limit curve is shifted by about 10% down.

### *3.2 Upper limit on $\alpha_L$ for strengthless bodies*

A solid body in a gravity regime (i.e., with zero or low tensile strength[7]) and with internal friction (angle of friction $\phi$) has an upper limit on $\alpha_L$ that can be given as an upper limit of $\alpha_L$ for a solid strengthless prolate spheroid ($a \geq b = c$) with the angle of friction $\phi$ (see Holsapple, 2001). It is

$$\alpha_{Lmax}(\phi) = \frac{L_c(\phi)}{L_{ceqsph}} = \frac{I\omega_c(\phi)}{I_{eqsph}\omega_{csph}}, \tag{18}$$

where $L_c(\phi)$ is the angular momentum of a critically spinning prolate spheroid, $L_{ceqsph}$ is the angular momentum of a critically spinning equivalent sphere (i.e., of the same mass and volume) with $\phi = 90°$, $I$ and $I_{eqsph}$ are their moments of inertia, and $\omega_c(\phi)$ and $\omega_{csph}$ are their critical spin rates.

The critical spin rate $\omega_c(90°)$ for a prolate spheroid ($a \geq b = c$) with the angle of friction $\phi = 90°$ has been derived by Richardson et al. (2005), they give a

[7] The population of asteroids larger than 0.3 km is predominated by bodies in a gravity regime, i.e., with a low (or zero) tensile strength that cannot rotate faster than the gravity spin limit; see Holsapple, 2006, and Pravec et al., 2006b.

formula

$$\omega_c(90^\circ) = \frac{\sqrt{2\pi\rho G}}{w^{3/2}} \sqrt{(w^2-1)\left[2w + ln\left(\frac{1-w}{1+w}\right)\right]}, \tag{19}$$

where $w \equiv \sqrt{1-(b/a)^2}$.

The critical spin rate $\omega_{csph}$ for a sphere with $\phi = 90^\circ$ is given by Eq. 16.

The moments of inertia are

$$I = \frac{1}{5} M(a^2 + b^2), \tag{20}$$

$$I_{eqsph} = \frac{2}{5} M a^2 \left(\frac{b}{a}\right)^{\frac{4}{3}}. \tag{21}$$

The ratio of the moments of inertia is

$$\frac{I}{I_{eqsph}} = \frac{1 - \frac{w^2}{2}}{(1-w^2)^{2/3}} \tag{22}$$

Substituting Eqs. 16, 19, and 22 into Eq. 18, we get a dependence of $\alpha_{Lmax}(90^\circ)$ on $a/b$. It is plotted in Fig. 1. It is also an upper limit for real bodies that deviate from the ideal ellipsoid (see Holsapple, 2001). Real asteroids have $a/b < 3$, so $\alpha_{Lmax}(90^\circ) < 1.37$. The angle of friction in real asteroids is unknown, but it is expected to be on an order of $40^\circ$ (Richardson et al., 2005). Holsapple (2001) calculated that $\omega_c(40^\circ)$ is about 10% lower than $\omega_c(90^\circ)$, so real asteroids in gravity regime (i.e., with low or zero tensile strength) have an upper limit on $\alpha_L$ from 0.9 to 1.3 for $a/b$ from 1.0 to 3.0.

## 4 Angular momentum content in binaries and related properties: Implications to binary formation theories

Data on the normalized total angular momentum $\alpha_L$ vs primary diameter $D_p$ for observed binaries are plotted in Fig. 2. These and other properties (commented below) suggest that there are three major binary populations (two of them may be related), and some outliers. The groupings are discussed in following paragraphs and they are presented also in Table 1. The table shows selected parameters of binaries for which we have useful estimates that illustrate characteristics of the groups described below. We point out that readers interested to work with the data should download the full dataset from the web site mentioned in Sect. 2, which contains more data and it also includes uncertainties, references, and notes.

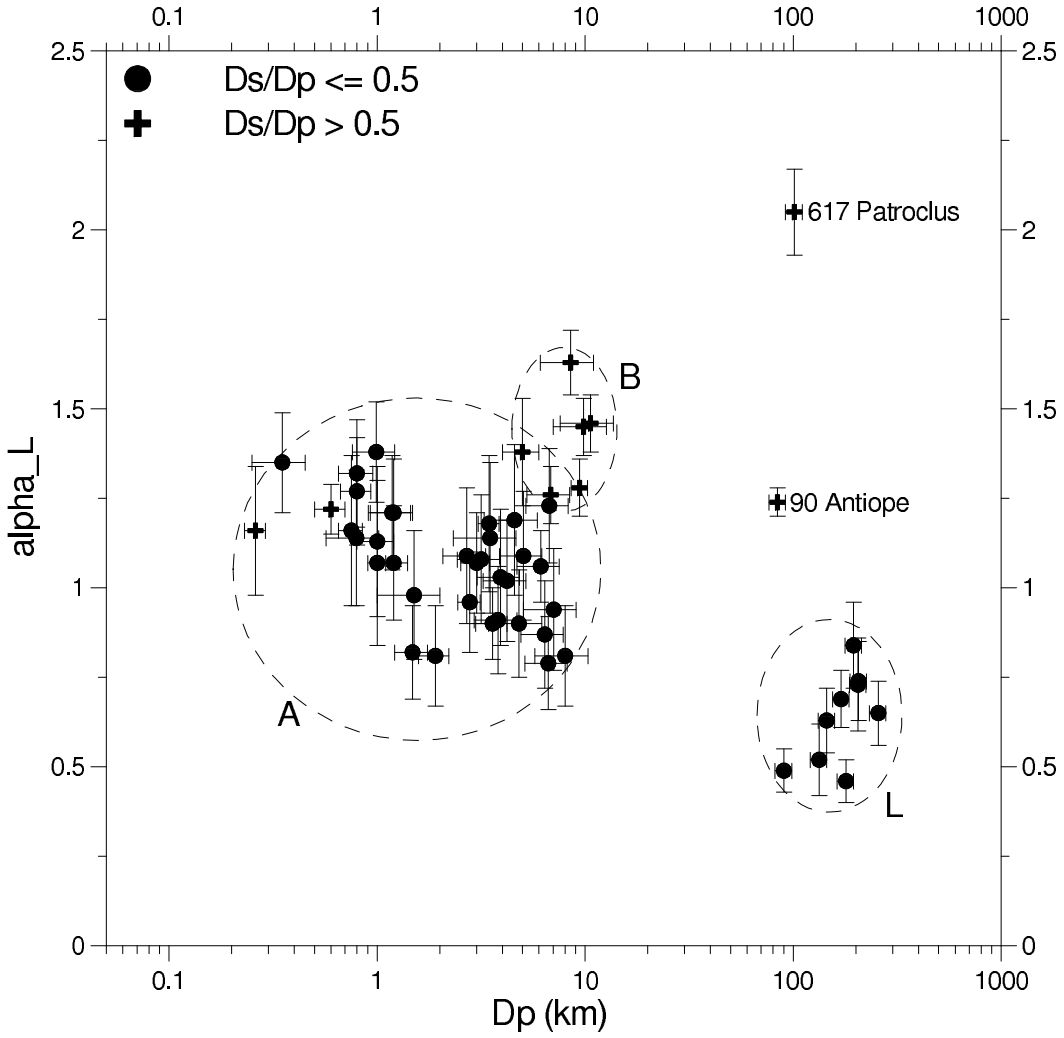


Fig. 2. Estimated $\alpha_L$ values vs $D_p$. The groups A+B are NEA/MC/small MB binaries. The group L are large asteroids with small satellites. Two exceptional cases are the two large double asteroids 90 Antiope and 617 Patroclus.

*Group L: Large asteroids with small satellites*

These are systems with $D_p$ from 90 to 270 km and $D_s/D_p$ from 0.02 to 0.21. (The lower limits for both parameters may be only observational detection limits and not real lower limits of the population.) They concentrate around $\alpha_L = 0.6$ in Fig. 2. A significance of the concentration is further apparent from Fig. 3 where data on primary rotation period vs diameter are plotted; primaries of the group L are relatively fast rotators with $P_{prim}$ from 4 to 7 hours. A comparison with spin data for all asteroids shows that primaries of the group L are actually among the fastest rotators in their size range. The observation of their narrow ranges of $\alpha_L$ and $P_{prim}$ should be a significant constraint for developing a theory of their formation; the currently preferred theory is that they were formed from ejecta from large asteroidal impacts (Durda et al. 2004), but their simulations did not constrain primary spins so far.

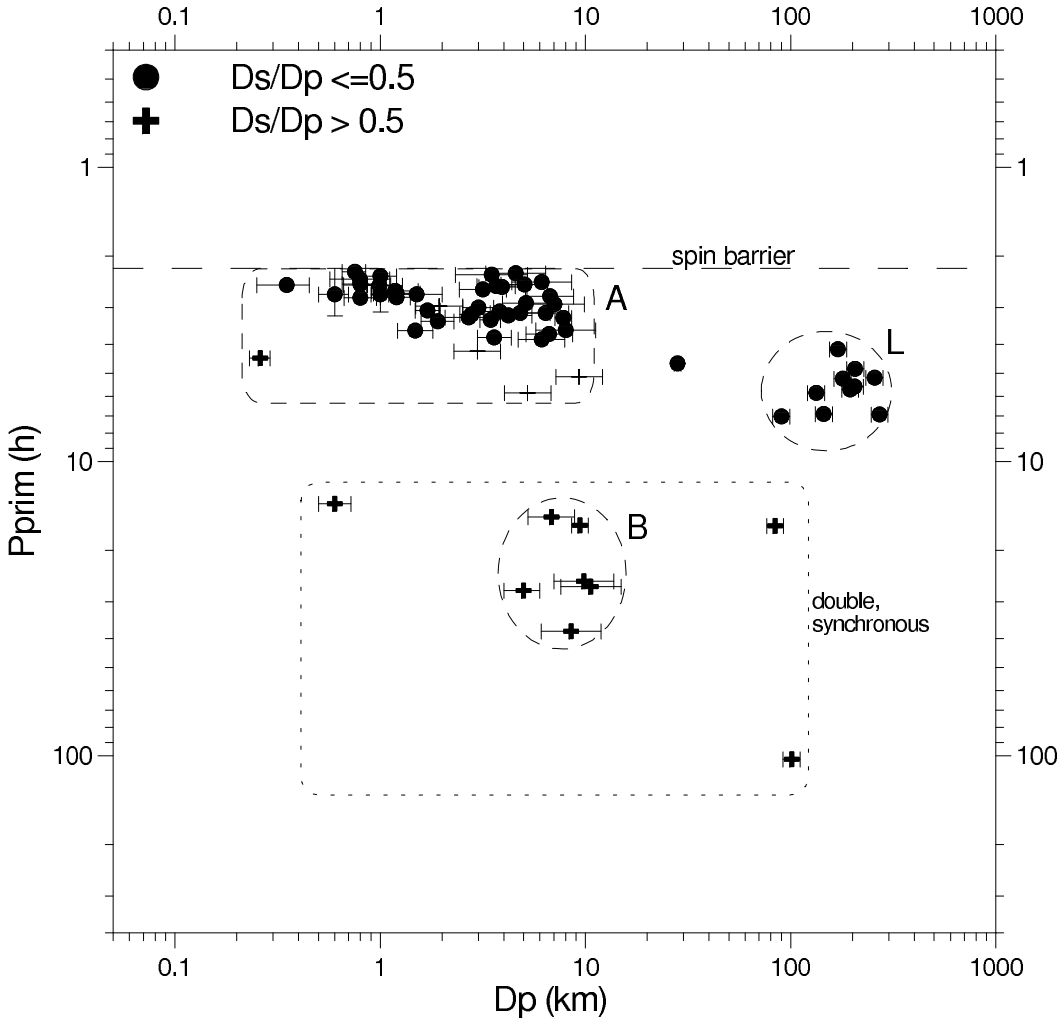


Fig. 3. Primary rotation period vs diameter. The groups A, B, and L are discussed in the text and caption of Fig. 2. Three synchronous double asteroids lie isolated in the plot: 69230 Hermes on the left and 90 Antiope and 617 Patroclus on the right side of the dotted box marking the synchronous double asteroids range; see text for comments on them.

*Group A+B: Small binaries with critical angular momentum content*
Binaries with $D_p$ about 10 km and smaller (group A+B) have $\alpha_L$ within error bars in the range 0.9-1.3, i.e., they have a total angular momentum very close to, but not generally exceeding, the critical limit for a single body in a gravity regime.[8] This suggests that the small binaries formed from parent bodies spinning at the critical rate (at the gravity spin limit for asteroids in the size range; see Pravec et al. 2006b) by some sort of fission or mass shedding. A candidate cause of spin-up to instability is the Yarkovsky-O'Keefe-Radzievskii-Paddack (YORP) effect, that we will discuss in Sect. 4.1.

There are seen two subgroups in the small binaries population. The subgroup A contains binary NEAs as well as small asynchronous MBA/MCs. The sub-

[8] Only one small binary, 854 Frostia, has estimated $\alpha_L = 1.63$ (uncertain by a factor of 1.06), which is about $4\sigma$ higher than the upper limit for a plausibly elongated single body.

group B consists of six synchronous main-belt binaries[9] with nearly equal size components ($D_s/D_p$ near 1) and with primary diameters about 10 km (Behrend et al. 2006, Kryszczyńska et al. 2005, Manzini et al. 2006). In Fig. 3 where data on $P_{prim}$ vs $D_p$ are plotted, the difference between the primary spins of the two subgroups is highlighted. Even though subgroup B appears distinct in the observed properties, it may be, however, only a tail of the population; the subgroup B binaries with size ratio close to 1 have much shorter tidal evolution time scales and therefore they may be just the most tidally evolved part of one population containing the subgroups A and B. This suggestion is supported by a tendency to slower primary spins with increasing $D_p$ in subgroup A that is apparent in Fig. 3, which is consistent with shorter tidal evolution time scales of larger binaries there.[10]

*(Sub)group W: Small wide binaries*
There are five small binaries ($D_p$ = 4–8 km) that have been detected with AO/HST and for which we have limited or no data to estimate the $\alpha_L$ values, but which are unique since they are wide binaries with $A/D_p$ on the order of tens. The primaries of two of the systems, 1509 Esclangona and 4674 Pauling, are fast rotators (Warner 2005, Warner et al. 2006), but the total angular momentum of the systems cannot be reasonably estimated since we do not know the orientations of their orbital angular momentum vectors. They may have formed from ejecta from large asteroidal impacts (like binaries in group L, albeit much smaller[11]), but more observations are needed to establish their properties so that they can be put into context with other binaries.

*Outliers: Large double asteroids 90 Antiope and 617 Patroclus*
Two large double asteroids appear unique. The Patroclus system has more angular momentum than could be contained in a single object. The Antiope system has $\alpha_L$ in the range that we observe in group A+B, but it is still higher than could be contained in a single object rotating not faster than similarly sized asteroids (which show the fastest rotations with periods of 4 h; cf. the normalized angular momentum of members of group L discussed above). They have not much prospect of having gained angular momentum since formation (too large and too distant for YORP). Thus, it seems that they may be examples of systems that simply formed as binaries, much as close binary stars do, from blobs of mass that simply have too much angular

[9] The one known synchronous, double asteroid among NEAs, 69230 Hermes, lies well inside subgroup A in Fig. 2, but it may actually be a very small member of subgroup B.
[10] Two points in the lower right corner of the dashed box marking the subgroup A in Fig. 3 are two asynchronous binaries, 1717 Arlon and 3982 Kastel, for which we have only limited data on their secondaries (but their $D_s/D_p$ values appear to be relatively large for subgroup A), and their longer primary rotation periods suggest that they may be the most tidally evolved ones among small asynchronous binaries, bridging a bit the gap between subgroups A and B.
[11] The large binary 379 Huenna, which is a member of group L, is actually a wide binary. It supports the idea that group W may be related to group L through the same formation mechanism.

momentum to condense into a single body. But "statistics of 2" is only slightly less dangerous than "statistics of one," so more data is needed to draw any significant conclusion.

### *4.1 Formation of small binaries with critical angular momentum content*

Small binary asteroids with $D_p$ about 10 km and smaller and with $\alpha_L$ in the critical range (group A+B) have properties so similar (some observed differences and trends might be due to size dependence of their evolution) that a search for a common formation mechanism is in order. We now look at how their properties compare with predictions from theories of binary formations.

Three general binary formation mechanisms have been proposed. The mechanism of binary formation from ejecta from large asteroidal impacts (Durda et al. 2004), which is supposed to form large/wide binaries with small satellites (groups L and W discusssed above), has not been shown to produce a total angular momentum for a system that is close to the critical amount that we observe in group A+B. The mechanism of tidal disruptions of strengthless bodies during close encounters with terrestrial planets (see Walsh and Richardson 2006, and references therein) obviously does not work in the main belt, so it cannot be a formation mechanism of small main belt binaries in the group A+B. The question of whether or not it might contribute to the NEA part of the population is discussed in the last paragraph of this section.

The critical angular momentum content of the group A+B binaries and their heliocentric orbit distribution ranging to the main belt favor the third proposed binary formation mechanism, which is a fission of or mass shedding by critically spinning parent bodies spun up by YORP (see Bottke et al. 2006, and references therein). Vokrouhlický et al. (2003) have shown convincingly that YORP has changed the spin rates and orientations of members of the Koronis family as large as ∼50 km in diameter by as much as ∼1 cycle per day per billion years. Since the rate of change of spin rate from YORP is inversely proportional to the square of the asteroid size, and also to the inverse-square of the heliocentric distance, a main-belt asteroid only 3 km in diameter can be spun up to instability in only ∼30 million years, and a 1-km diameter near-Earth asteroid in only about one million years. Thus, the YORP effect is powerful enough to spin up small asteroids to fission or mass shedding in a time much shorter than their lifetimes (see also discussion below). However, the binary systems are observed to have no more than just the critical angular momentum, so if YORP spin-up is the cause, then it must be shut off promptly after the formation of a binary. Unlike other wider binaries, the primaries of these systems show only small deviations from rotational symmetry, as revealed by radar and their low amplitude primary lightcurves. The secondaries, on the other hand, are often quite elongated, enough so that their lightcurve variation is often apparent, even when diluted by an order of magnitude by the light of the primary.

Table 1
Selected binary asteroids parameters

| Binary system | $D_p$(km) | $D_s/D_p$ | $P_{prim}$(h) | $P_{orb}$(h) | $P_{sec}$(h) | $A/D_p$ | $\alpha_L$ | $q_h$(AU) | $a_h$(AU) |
|---|---|---|---|---|---|---|---|---|---|
| Group L: | | | | | | | | | |
| (22) Kalliope | 170 | 0.213 | 4.1482 | 86.16 | | 6.3 | 0.69 | 2.610 | 2.909 |
| (45) Eugenia | 195 | 0.036 | 5.6991 | 114.38 | | 6.1 | 0.84 | 2.497 | 2.720 |
| (87) Sylvia | 256 | 0.063 | 5.1836 | 87.59 | | 5.3 | 0.65 | 3.212 | 3.490 |
| (107) Camilla | 206 | 0.050 | 4.8439 | 89.04 | | 6.0 | 0.74 | 3.204 | 3.478 |
| (121) Hermione | (205) | 0.066 | 5.5513 | 61.97 | | (3.7) | 0.73 | 2.967 | 3.453 |
| (130) Elektra | 179 | 0.026 | 5.225 | (94.1) | | (7.0) | (0.46) | 2.463 | 3.122 |
| (283) Emma | 145 | 0.079 | 6.888 | 80.74 | | 4.1 | 0.63 | 2.578 | 3.042 |
| (379) Huenna | 90 | 0.078 | (7.022) | 1939 | | 38 | 0.49 | 2.532 | 3.130 |
| (762) Pulcova | 133 | 0.16 | 5.839 | 96 | | 6.1 | 0.52 | 2.855 | 3.160 |
| Group A: | | | | | | | | | |
| (1862) Apollo | 1.7 | 0.04 | 3.0662 | | | | | 0.647 | 1.471 |
| (2006) Polonskaya | 6.4 | (0.23) | (3.1179) | 19.15 | | (2.1) | (0.87) | 1.874 | 2.324 |
| (2044) Wirt | 7 | 0.25 | 3.6897 | 18.97 | (18.97) | (2.1) | 0.79 | 1.569 | 2.382 |
| (2754) Efimov | 6 | 0.20 | 2.4497 | 14.765 | | (1.8) | 1.08 | 1.711 | 2.228 |
| (3309) Brorfelde | 5.0 | 0.26 | 2.5041 | 18.48 | 18.47 | (2.0) | 1.09 | 1.721 | 1.818 |
| (3671) Dionysus | 1.5 | 0.2 | 2.7053 | 27.74 | | (2.7) | 0.98 | 1.007 | 2.198 |
| (3703) Volkonskaya | 2.7 | 0.4 | 3.235 | (24) | | (2.5) | (1.09) | 2.019 | 2.332 |
| (3782) Celle | 6 | 0.43 | 3.839 | 36.57 | | (3.3) | 1.06 | 2.187 | 2.415 |
| (4029) Bridges | 8 | 0.24 | 3.5746 | 16.31 | | (1.9) | 0.81 | 2.190 | 2.525 |
| (4786) Tatianina | 7 | 0.19 | 2.9227 | 21.67 | | (2.3) | 0.94 | 1.904 | 2.359 |
| (5381) Sekhmet | 1.0 | 0.30 | 2.7 | 12.5 | 10 | 1.54 | 1.07 | 0.667 | 0.947 |
| (5407) 1992 AX | 3.9 | (0.2) | (2.5488) | (13.520) | | (1.7) | (1.03) | 1.328 | 1.838 |
| (5477) 1989 UH2 | 3.0 | 0.37 | 2.9941 | 24.42 | | (2.5) | 1.07 | 1.772 | 1.917 |
| (5905) Johnson | 3.6 | 0.38 | 3.7824 | 21.785 | | (2.3) | 0.90 | 1.773 | 1.910 |
| (6084) Bascom | 7 | 0.37 | 2.7454 | 43.5 | 43.5 | (3.7) | 1.23 | 1.767 | 2.313 |
| (7088) Ishtar | 1.2 | 0.42 | 2.6787 | 20.63 | 20.60 | (2.2) | 1.21 | 1.209 | 1.981 |
| (9260) Edwardolson | 3.8 | 0.27 | 3.0854 | 17.785 | | (2.0) | 0.91 | 1.763 | 2.290 |
| (9617) Grahamchapman | 5 | 0.27 | 2.2856 | 19.385 | | (2.1) | 1.19 | 1.973 | 2.224 |
| (11264) Claudiomaccone | 4.2 | 0.4 | 3.1872 | 15.11 | | (1.8) | 1.02 | 1.983 | 2.581 |
| (17260) 2000 JQ58 | 5 | 0.26 | 3.1287 | 14.757 | 14.75 | (1.8) | 0.90 | 1.800 | 2.204 |
| (34706) 2001 OP83 | 3.2 | 0.28 | 2.5944 | 20.76 | | (2.2) | 1.08 | 1.395 | 2.254 |
| (35107) 1991 VH | 1.2 | 0.38 | 2.6237 | 32.67 | (12.836) | (3.0) | 1.21 | 0.973 | 1.136 |
| (65803) Didymos | 0.75 | 0.22 | 2.2593 | 11.91 | (11.91) | (1.5) | 1.16 | 1.013 | 1.644 |
| (66063) 1998 RO1 | 0.8 | 0.48 | 2.4924 | 14.54 | 14.52 | (1.8) | 1.32 | 0.277 | 0.991 |
| (66391) 1999 KW4 | 1.282 | 0.330 | 2.7645 | 17.422 | (17.422) | 1.99 | 1.06 | 0.200 | 0.642 |
| (76818) 2000 RG79 | 2.8 | 0.35 | 3.1665 | 14.127 | 14.127 | (1.7) | 0.96 | 1.745 | 1.930 |
| (85938) 1999 DJ4 | 0.35 | 0.5 | 2.5141 | 17.73 | (17.73) | (2.1) | 1.35 | 0.957 | 1.852 |
| (88710) 2001 SL9 | 0.8 | 0.28 | 2.4004 | 16.40 | | (1.9) | 1.14 | 0.775 | 1.061 |
| 1994 AW1 | 1.0 | 0.49 | 2.5193 | 22.3 | | (2.4) | 1.38 | 1.021 | 1.105 |
| 1996 FG3 | 1.5 | 0.31 | 3.5942 | 16.14 | (16.15) | (1.9) | 0.82 | 0.685 | 1.054 |
| 1999 HF1 | 3.5 | 0.23 | 2.31927 | 14.03 | (14.03) | (1.7) | 1.14 | 0.440 | 0.819 |
| 2000 DP107 | 0.8 | 0.41 | 2.7754 | 42.12 | 42.2 | (3.6) | 1.27 | 0.851 | 1.366 |
| 2000 UG11 | 0.26 | 0.58 | 4.44 | 18.4 | | (2.2) | 1.16 | 0.827 | 1.929 |
| 2002 CE26 | 3.45 | 0.09 | 3.2930 | 15.6 | (15.6) | 1.36 | 1.18 | 0.985 | 2.234 |
| 2003 YT1 | 1.0 | 0.18 | 2.343 | 30 | | (2.8) | 1.13 | 0.786 | 1.110 |
| 2005 AB | 1.9 | 0.24 | 3.339 | 17.93 | | (2.0) | 0.81 | 1.107 | 3.216 |
| Group B: | | | | | | | | | |
| (809) Lundia | 7 | 0.9 | (15.4) | 15.4 | (15.4) | (2.2) | 1.26 | 1.843 | 2.283 |
| (854) Frostia | 9 | 0.98 | (37.711) | 37.711 | (37.711) | (4.1) | 1.63 | 1.957 | 2.368 |
| (1089) Tama | 9.4 | 0.9 | (16.444) | 16.444 | (16.444) | (2.3) | 1.28 | 1.930 | 2.214 |
| (1139) Atami | 5 | 0.8 | (27.45) | 27.45 | (27.45) | (3.1) | 1.38 | 1.450 | 1.947 |
| (1313) Berna | 10 | 0.97 | (25.464) | 25.464 | (25.464) | (3.1) | 1.45 | 2.107 | 2.657 |
| (4492) Debussy | 11 | 0.93 | (26.606) | 26.606 | (26.606) | (3.2) | 1.46 | 2.270 | 2.766 |
| (69230) Hermes | 0.6 | 0.9 | (13.894) | 13.894 | (13.894) | (2.0) | 1.22 | 0.622 | 1.655 |
| Group W: | | | | | | | | | |
| (1509) Esclangona | 7.8 | 0.33 | 3.247 | (874) | | (27) | | 1.806 | 1.866 |
| (3749) Balam | 6 | 0.22 | | 2640 | | (56) | | 1.992 | 2.237 |
| (4674) Pauling | 3.7 | 0.32 | 2.5306 | (3550) | | (68) | | 1.728 | 1.859 |
| (17246) 2000 GL74 | 4.2 | 0.40 | | 2034 | | (48) | | 2.781 | 2.839 |
| (22899) 1999 TO14 | 4.3 | 0.32 | | 1356 | | (36) | | 2.602 | 2.843 |
| Outliers — Large double synchronous asteroids: | | | | | | | | | |
| (90) Antiope | 84 | 0.97 | (16.51) | 16.51 | (16.51) | 2.02 | 1.24 | 2.664 | 3.156 |
| (617) Patroclus | 101 | 0.92 | (102.8) | 102.8 | | 6.7 | 2.05 | 4.506 | 5.227 |

A pair of papers just published by Ostro et al. (2006) and Scheeres et al. (2006) provide profound insight into how small asynchronous binaries might evolve into their present states. They report detailed radar imaging of the binary NEA (66391) 1999 $KW_4$, and a detailed dynamical description of the system. The images of the primary reveal a top-shaped object, with an equatorial profile that deviates no more than a few percent from circular. Indeed, the equatorial band appears as if it has been planed smooth by some process. Even more remarkable, the spin of the primary is only 1.3% slower than the critical rate at which a particle on the equator would levitate from the surface and go into orbit. It seems unlikely that such a close match to critical spin is a mere coincidence. The secondary, which rotates synchronously with the orbit period, is far more irregular, in fact with a shape roughly similar to the gravitational Roche lobe surrounding it.

It is not clear yet how a slowly accelerating "rubble pile" becomes a binary, whether by slowly shedding mass at the equator or by a "landslide" event that spontaneously leads to a fissioned binary. In either case, one can imagine that the newly formed binary (after the slowly shed mass accumulates into a significant secondary, if it happens that way) still has the primary spinning rapidly with the satellite outside of the synchronous orbit radius, and thus in a longer period orbit. Initially, if the primary is spinning essentially at the critical spin rate, as 1999 $KW_4$ is now, the tidal attraction of the satellite will suffice to literally pick matter up off the surface at the equator as it passes under the satellite. Material so levitated will not escape into orbit, but instead will be re-deposited behind the location where it was lifted from, and in the process will transfer torque to the satellite, thus slowing the spin of the primary and evolving the satellite orbit outward. This process is exactly analogous to tidal friction, but because it involves actual mass transport over substantial distances instead of just elastic energy dissipation from minuscule displacements, it can be expected to act orders of magnitude faster. In the process of moving matter about along the equator, this process also serves to "pave" the equator into an extremely regular profile. This process of regularizing the figure of the primary should also serve to shut off the YORP acceleration to a large degree, so that the system will stall out rather than continuing to gain angular momentum.

What we describe in the above paragraph is, so far, a bit of a Kipling-style "just so story", which fits all of the observational details of the radar observations, but is in need of detailed modeling to confirm (or refute) the picture. Perhaps as important as explaining the dynamical configuration of 1999 $KW_4$ is the fact that the general characteristics of the other small asynchronous binaries are similar to 1999 $KW_4$ in having spins close to the critical limit and near-circular equatorial profiles, as revealed by lightcurve and/or radar data. See, for example, the similar, even if less detailed, images of 2002 $CE_{26}$ in the paper by Shepard et al. (2006). Thus, 1999 $KW_4$ may be the archetype for the class, and its strange dynamical state may be "the way nature works" for all of these members of the group A.

A question is whether or not the fission of asteroids spun up by the YORP

effect is also a formation mechanism of synchronous double asteroids in the group B that have critical angular momentum content as well. If there are found evolved asynchronous binaries with large secondaries and with primary spins slowed down a lot from presumed initial fast rotations, that would bridge the "gap" between the two groups in the parameter space –two candidate systems have been mentioned above– it would further support our suggestion that the groups A and B may be actually parts of one population. Future observations with techniques and strategies developed so as to suppress the present observational selection effect against detection of such evolved asynchronous binaries with longer periods may bring such needed data.

An important thing requiring further study is how the NEA part of the binary population has been affected by tidal interactions during close approaches to the terrestrial planets. Walsh and Richardson (2007) simulated a steady-state binary NEA population, and they found that tidal disruptions could account for only 1–2% of NEAs being binary. They estimated a lifetime of typical NEA binaries due to disruptions during close approaches to Earth and Venus to be only 1–2 Myr, and they found that it strongly depends on binary semi-major axis. The estimated binary survival lifetime is much shorter than the median lifetime of NEAs in their heliocentric orbits that is around 10 Myr (Gladman et al. 2000). This implies that binaries formed in and transported from the main belt may be only a small part of the NEA binary population, and that the NEA binaries mostly formed after their parents were transported from the main belt. The strong dependence of the lifetime of NEA binaries on separation of components may be an explanation for the fact that the NEA binaries show the tendency to smaller separations (shorter periods), but it may be also a size effect (discussed above) as our sample of MBA binaries contains objects larger than most NEA binaries. In any case, if binary NEAs are so short living and they disrupt so frequently, the formation mechanism (presumably YORP) must form new NEA binaries on a shorter timescale so that the fraction of binaries among NEAs remains so high ($\sim 15\%$) as observed. Since strength of the YORP effect is inversely proportional to the square of diameter, and a 1-km diameter near-Earth asteroid can be spun up to instability in about 1 Myr, the binary fraction in the NEA population may show a size dependence. Indeed, Pravec et al. (2006a) found that binary systems concentrate among NEAs smaller than 2 km in diameter and that the fraction of binaries decreases significantly among larger NEAs. That "upper limit" on binary sizes is not being observed among the small MBA binaries of the group A+B. So, the data seem to be consistent with the short lifetime and its strong dependence on semi-major axis of the NEA binaries found by Walsh and Richardson (2007). The question then occurs, what becomes of the disrupted NEA binaries? Tidal disruptions do not change the primary spin rate by very much, so either the disrupted binaries "recycle" themselves, or we are left with an excess of single fast rotators. More than half of fastest rotating NEAs larger than 0.3 km with periods between 2.2 and 2.8 h are probably binaries (Pravec et al. 2006a), so maybe the disrupted binary primaries indeed form new binaries.

# APPENDIX

## A Diameter, albedo, and absolute magnitude relation

The geometric albedo $p$ is defined as

$$p \equiv \frac{F_{obj}(0,\Delta)}{F(0,\Delta)}, \tag{A.1}$$

where $F_{obj}(0,\Delta)$ is the light flux from the object at zero phase angle, $F(\alpha,\Delta) \equiv F(0,\Delta)\cos\alpha$ is the light flux from a geometrically scattering white planar surface of area $S$ at phase angle $\alpha$, $S$ is cross section of the object, and $\Delta$ is observer's distance.

Amount of light scattered from the white planar surface is equal to the amount of incident light:

$$\int_0^{2\pi}\int_0^{\pi/2} F(\alpha,\Delta)\Delta^2 \sin\alpha \, \mathrm{d}\alpha \, \mathrm{d}\phi = F_0 S, \tag{A.2}$$

where $F_0$ is incident light flux.

Substituting $S \equiv \pi D^2/4$, where $D$ is an effective diameter of the object, and calculating the definite integral, we get

$$p = \frac{4\Delta^2}{D^2}\frac{F_{obj}(0,\Delta)}{F_0}. \tag{A.3}$$

The absolute magnitude, $H$, of a solar system object is defined as the apparent magnitude of the object illuminated by the solar light flux at 1 AU and observed from the distance of 1 AU and at zero phase angle. From that, we get

$$H = V_{sun} - 2.5\log\frac{F_{obj}(0,1\mathrm{AU})}{F_0}, \tag{A.4}$$

where $V_{sun}$ is the apparent magnitude of the Sun at 1 AU.

From Eqs. A.3 and A.4, we get the final relation

$$D\sqrt{p} = K \cdot 10^{-H/5}, \tag{A.5}$$

where

$$K \equiv 2 \text{ AU} \cdot 10^{V_{sun}/5}. \tag{A.6}$$

The derivation above is independent of a magnitude system used. The zero point of the magnitude system enters there through the apparent magnitude of the Sun. The value of $V_{sun}$ is to be taken from solar/stellar works. For the absolute magnitudes of asteroids, the Johnson V band is used as the standard. Campins et al. (1985) estimated $V_{sun} = -26.762 \pm 0.017$. This translates to a value for $K$ of $1329 \pm 10$ km, which is the value that was used for estimating diameters within the IRAS Minor Planet Survey (Fowler and Chillemi, 1992) as well as many subsequent works, and we use it in our work as well. The uncertainty of the $V_{sun}$ value may cause a systematic error of about 1% in asteroid diameter estimates, which is smaller than other uncertainties that come into play when making those estimates.

## Acknowledgements

The work at Ondřejov was supported by the Grant Agency of the Czech Republic, Grant 205/05/0604. The work at Space Science Institute (A.W.H.) was supported by grant NAG5-13244 from the NASA Planetary Geology-Geophysics Program. P.P. did a part of the work during his stay at *Institut de mécanique céleste et de calcul des éphémérides (IMCCE)* in Paris in June 2006. We thank to A. Galád for assistance with the binary data compilation.

### References

Behrend, R., and 48 colleagues, 2006. Four new binary minor planets: (854) Frostia, (1089) Tama, (1313) Berna, (4492) Debussy. Astron. Astrophys. 446, 1177–1184.

Belton, M.J.S., Chapman, C.R., Klaasen, K.P., Harch, A.P., Thomas, P.C., Veverka, J., McEwen, A.S., Pappalardo, R.T., 1996. Galileo's Encounter with 243 Ida: an Overview of the Imaging Experiment. Icarus 120, 1-19.

Benner, L.A.M., Nolan, M.C., Margot, J.-L., Ostro, S.J., Giorgini, J.D., 2003. Radar Imaging of Binary Near-Earth Asteroid 1998 ST27. Bull. Amer. Astron. Soc. 35, 959.

Benner, L.A.M., Nolan, M.C., Ostro, S.J., Giorgini, J.D., Margot, J.-L., Magri, C., 2005. 1994 XD. IAU Circ. 8563.

Benner, L.A.M., Nolan, M.C., Shepard, M.K., Giorgini, J.D., Ostro, S.J., Busch, M.W., Hine, A. A., 2006. 2006 GY2. CBET 534.

Binzel, R.P., Slivan, S.M., Magnusson, P., Wisniewski, W.Z., Drummond, J., Lumme, K., Barucci, M.A., Dotto, E., Angeli, C., Lazzaro, D., 1993. Asteroid 243 Ida - Groundbased photometry and a pre-Galileo physical model. Icarus 105, 310–325.

Bottke, W.F. Jr., Vokrouhlický, D., Rubincam, D.P., Nesvorný, D., 2002. The Yarkovsky and YORP effects: Implications for asteroid dynamics. Ann. Rev.

Earth Planet. Sci. 34, 157–191.

Brown, M.E., Margot, J.-L., 2001. S/2001 (87) 1. IAU Circ. 7588.

Campins, H., Rieke, G.H., Lebofsky, M.J., 1985. Absolute calibration of photometry at 1 through 5 $\mu$m. Astron. J. 90, 896–899.

Chapman, C.R., and 11 colleagues, 1995. Discovery and physical properties of Dactyl, a satellite of asteroid 243 Ida. Nature 374, 783–785.

Cooney, W., Gross, J., Terrell, D., Stephens, R., Pravec, P., Kušnirák, P., Durkee, R., Galád, A., 2006a. (1717) Arlon. CBET 369.

Cooney, W., and 16 colleagues, 2006b. (1717) Arlon. CBET 504.

Davis, R.G., 2001. High precision lightcurves for 762 Pulcova. Minor Planet Bull. 28, 10-12.

Delbó, M., Harris, A. W., Binzel, R. P., Pravec, P., Davies, J. K., 2003. Keck observations of near-Earth asteroids in the thermal infrared. Icarus 166, 116-130.

Durda, D.D., Bottke, W.F. Jr., Enke, B.L., Merline, W.J., Asphaug, E., Richardson, D.C., Leinhardt, Z.M., 2004. The formation of asteroid satellites in large impacts: results from numerical simulations. Icarus 170, 243–257.

Fernández, Y.R., Sheppard, S.S., Jewitt, D.C., 2003, The albedo distribution of Jovian Trojan asteroids. Astron. J. 126, 1563-1574.

Florczak, M., Lazzaro, D., Duffard, R., 2002. Discovering new V-type asteroids in the vicinity of 4 Vesta. Icarus 159, 178-182.

Fowler, J.W., Chillemi, J.R., 1992. IRAS asteroid data processing. In *The IRAS Minor Planet Survey* (E. F. Tedesco, G. J. Veeder, J. W. Fowler, and J. R. Chillemi, eds.) Phillips Laboratory, PL-TR-92-2049, Hanscom AFB, MA. pp.17-43.

Gladman, B., Michel, P., Froeschlé, C., 2000. The near-Earth object population. Icarus 146, 176–189.

Hansen, A.T., Arentoft, T., Lang, K., 1997. The rotational period of 90 Antiope. Minor Planet Bull. 24, 17.

Harris, A.W., Young, J.W., Goguen, J., Hammel, H.B., Hahn, G., Tedesco, E.F., Tholen, D.J., 1987. Photoelectric lightcurves of the asteroid 1862 Apollo. Icarus 70, 246-256.

Harris, A.W., Young, J.W., Dockweiler, T., Gibson, J., Poutanen, M., Bowell, E., 1992. Asteroid lightcurve observations from 1981. Icarus 95, 115-147.

Helfenstein, P., and 10 colleagues, 1996. Galileo photometry of asteroid 243 Ida. Icarus 120, 48-65.

Higgins, D., Pravec, P., Kušnirák, P., Šarounová, L., Gajdoš, Š., Galád, A., Világi, J., 2006a. (6084) Bascom. CBET 389.

Higgins, D., Pravec, P., Kušnirák, P., Galád, A., Gajdoš, Š., Világi, J., Kornoš, L., 2006b. (17260) 2000 $JQ_{58}$. CBET 431.

Higgins, D., Pravec, P., Kušnirák, P., Cooney, W., Gross, J., Terrell, D., Stephens, R., 2006c. (4029) Bridges. CBET 507.

Holsapple, K.A., 2001. Equilibrium configurations of solid cohesionless bodies. Icarus 154, 432–448.

Holsapple, K.A., 2006. Spin limits of Solar System bodies: From the small fast-rotators to 2003 EL61. Icarus, in press.

Jakubík, M., and 11 colleagues, 2005. (9260) Edwardolson. CBET 270.

Kaasalainen, M., Torppa, J., Muinonen, K., 2001. Optimization methods for asteroid lightcurve inversion. II. The complete inverse problem. Icarus 153, 37-51.

Kaasalainen, M., Torppa, J., Muinonen, K., 2002. Models of twenty asteroids from photometric data. Icarus 159, 369-395.

Krugly, Yu.N., Maccone, C., Gaftonyuk, N.M., Lupishko, D.F., Shevchenko, V.G., Velichko, F.P., 2006. 11264 Claudiomaccone: Small binary main-belt asteroid. Planet. Space Sci., in press.

Kryszczyńska, A., Kwiatkowski, T., Hirsch, R., Polinska, M., Kaminski, K., Marciniak, A., 2005. (809) Lundia. CBET 239.

Larson, S.M., and 12 colleagues, 2004. Physical characteristics of the binary PHA 2003 YT1. Bull. Amer. Astron. Soc. 36, 139.

Magnusson, P., 1990. Spin vectors of 22 large asteroids. Icarus 85, 229-240.

Manzini, F., and 27 colleagues, 2006. (1139) Atami. CBET 430.

Marchis, F., Descamps, P., Berthier, J., Hestroffer, D., de Pater, I., Conrad, A., Le Mignant, D., Chaffee, F., Gavel, D., 2003a. Searching and studying binary asteroids with AO systems. Bull. Amer. Astron. Soc. 35, 959.

Marchis, F., Descamps, P., Hestroffer, D., Berthier, J., Vachier, F., Boccaletti, A., de Pater, I., Gavel, D., 2003b. A three-dimensional solution for the orbit of the asteroid satellite of 22 Kalliope. Icarus 165, 112-120.

Marchis, F., Laver, C., Berthier, J., Descamps, P., Hestroffer, D., de Pater, I., Behrend, R., Roy, R., Baudoin, P., 2004a. (121) Hermione. IAU Circ. 8264.

Marchis, F., Descamps, P., Hestroffer, D., Berthier, J., de Pater, I., 2004b. Fine analysis of 121 Hermione, 45 Eugenia, and 90 Antiope binary asteroid systems with AO observations. Bull. Amer. Astron. Soc. 36, 1180.

Marchis, F., Descamps, P., Hestroffer, D., Berthier, J., 2005. Discovery of the triple asteroidal system 87 Sylvia. Nature 436, 822-824.

Marchis, F., and 17 colleagues, 2006a. A low density of 0.8 gcm$^{-3}$ for the Trojan binary asteroid 617 Patroclus. Nature 439, 565-567.

Marchis, F., Kaasalainen, M., Hom, E.F.Y., Berthier, J., Enriquez, J., Hestroffer, D., Le Mignant, D., de Pater, I., 2006b. Shape, size and multiplicity of main-belt asteroids I. Keck adaptive optics survey. Icarus, in press.

Marchis, F., Wong, M. H., Berthier, J., Descamps, P., Hestroffer, D., Vachier, F., Le Mignant, D., Keck Observatory, W. M., de Pater, I., 2006c. S/2006 (624) 1. IAU Circ. 8732.

Margot, J.-L., 2003. S/2003 (379) 1. IAU Circ. 8182.

Margot, J.-L., Brown, M.E., 2003. A low-density M-type asteroid in the main belt. Science 300, 1939–1942.

Margot, J.-L., Nolan, M.C., Benner, L.A.M., Ostro, S.J., Jurgens, R.F., Giorgini, J.D., Slade, M.A., Campbell, D.B., 2002. Binary asteroids in the near-Earth object population. Science 296, 1445-1448.

Merline, W.J., Close, L.M., Dumas, C., Shelton, J.C., Menard, F., Chapman, C.R., Slater, D.C., 2000. Discovery of companions to asteroids 762 Pulcova and 90 Antiope by direct imaging. Bull. Amer. Astron. Soc. 32, 1017.

Merline, W.J., Weidenschilling, S.J., Durda, D.D., Margot, J.-L., Pravec, P., Storrs, A.D., 2002. Asteroids do have satellites. In: Bottke Jr., W.F., Cellino, A., Paolicchi, P., Binzel, R.P. (Eds.), Asteroids III, Univ. of Ariz. Press, Tucson, pp. 289–312.

Merline, W.J., Close, L.M., Tamblyn, P.M., Menard, F., Chapman, C.R., Dumas, C., Duvert, G., Owen, W.M., Slater, D.C., Sterzik, M.F., 2003a. S/2003 (1509) 1. IAU Circ. 8075.

Merline, W.J., Dumas, C., Siegler, N., Close, L.M., Chapman, C.R., Tamblyn, P.M., Terrell, D., Conrad, A., Menard, F., Duvert, G., 2003b. S/2003 (283) 1. IAU Circ. 8165.

Merline, W.J., Tamblyn, P.M., Dumas, C., Close, L.M., Chapman, C.R., Menard, F., 2003c. S/2003 (130) 1. IAU Circ. 8183.

Merline, W.J., Tamblyn, P.M., Chapman, C.R., Nesvorný, D., Durda, D.D., Dumas, C., Storrs, A.D., Close, L.M., Menard, F., 2003d. S/2003 (22899) 1. IAU Circ. 8232.

Merline, W.J., Tamblyn, P.M., Dumas, C., Menard, F., Close, L.M., Chapman, C.R., Duvert, G., Ageorges, N., 2004. S/2004 (4674) 1. IAU Circ. 8297.

Michałowski, T., and 14 colleagues, 2004. Eclipsing binary asteroid 90 Antiope. Astron. Astrophys. 423, 1159-1168.

Neish, C.D., Nolan, M.C., Howell, E.S., Rivkin, A.S., 2003. Radar observations of binary asteroid 5381 Sekhmet. Bull. Amer. Astron. Soc. 35, 1421.

Nolan, M.C., Howell, E.S., Magri, C., Beeney, B., Campbell, D.B., Benner, L.A.M., Ostro, S.J., Giorgini, J.D., Margot, J.-L., 2002a. 2002 $BM_{26}$. IAU Circ. 7824.

Nolan, M.C., Howell, E.S., Ostro, S.J., Benner, L.A.M., Giorgini, J.D., Margot, J.-L., Campbell, D.B., 2002b. 2002 $KK_8$. IAU Circ. 7921.

Nolan, M.C., Hine, A.A., Howell, E.S., Benner, L.A.M., Giorgini, J.D., 2003. 2003 $SS_{84}$. IAU Circ. 8220.

Ostro, S.J., Rosema, K.D., Campbell, D.B., Shapiro, I.I., 2002. Radar observations of asteroid 1862 Apollo. Icarus 156, 580-583.

Ostro, S.J., Nolan, M.C., Benner, L.A.M., Giorgini, J.D., Margot, J.-L., Magri, C., 2003. 1990 OS. IAU Circ. 8237.

Ostro, S.J., Benner, L.A.M., Giorgini, J.D., Nolan, M.C., Hine, A.A., Howell, E.S., Margot, J.-L., Magri, C., Shepard, M.K., 2005. (1862) Apollo. IAU Circ. 8627.

Ostro, S.J., and 15 colleagues, 2006. Asteroid 66391 (1999 KW4): Radar images and a physical model of a near-Earth binary system. Science, in press.

Petit, J.-M., Durda, D.D., Greenberg, R., Hurford, T.A., Geissler, P.E., 1997. The long-term dynamics of Dactyl's orbit. Icarus 130, 177-197.

Pravec, P., and 10 colleagues, 2000. Two-period lightcurves of 1996 $FG_3$, 1998 PG, and (5407) 1992 AX: One probable and two possible binary asteroids. Icarus 146, 190-203.

Pravec, P., and 56 colleagues, 2006a. Photometric survey of binary near-Earth asteroids. Icarus 181, 63-93.

Pravec, P., Harris, A.W., Warner, B., 2006b. NEA rotations and binaries. In: Milani, A., Valsecchi, G.B., Vokrouhlický, D. (Eds.), Proceedings of the IAU Symposium 236, in press.

Pray, D., Pravec, P., Kušnirák, P., Cooney, W., Gross, J., Terrell, D., 2005a. (2006) Polonskaya. IAU Circ. 8630.

Pray, D., Pravec, P., Kušnirák, P., Gajdoš, Š., Világi, J., Galád, A., Nudds, S., Krzeminski, Z., 2005b. (114319) 2002 $XD_{58}$. CBET 328.

Pray, D., Pravec, P., Kušnirák, P., Cooney, W., Gross, J., Terrell, D., Galád, A., Gajdoš, Š., Világi, J., Durkee, R., 2006. (2044) Wirt. CBET 353.

Pray, D., Pravec, P., Kušnirák, P., Reddy, V., Dyvig, R., Gajdoš, Š., 2006b. (9617) Grahamchapman. CBET 414.

Pray, D., Pravec, P., Kušnirák, P., Nudds, S., Galád, A., Gajdoš, Š., Világi, J., Koff, R., 2006c. (4786) Tatianina. CBET 472.

Pray, D., Pravec, P., Pikler, M., Husárik, M., Stephens, R., Masi, G., Durkee, R., Goncalves, R., 2006d. (2754) Efimov. CBET 617.

Reddy, V., Dyvig, R., Pravec, P., Kušnirák, P., Gajdoš, Š., Galád, A., Kornoš, L., 2006a. (7088) Ishtar. CBET 384.

Reddy, V., and 13 colleagues, 2006b. Photometric and radar observations of 2005 AB: A new binary near-Earth asteroid. 37nd Annual Lunar and Planetary Science Conference, March 13-17, 2006, League City, Texas, abstract no. 1755.

Richardson, D.C., Elankumaran, P., Sanderson, R.E., 2005. Numerical experiments with rubble piles: equilibrium shapes and spins. Icarus 173, 349–361.

Ryan, W.H., Ryan, E.V., Martinez, C.T., 2004a. 3782 Celle: Discovery of a binary system within the Vesta family of asteroids. Planet. Space Sci. 52, 1093-1101.

Ryan, W.H., Ryan, E.V., Martinez, C.T., 2004b. Unusual lightcurves in the Vesta family of asteroids. Bul. Amer. Astron. Soc. 36, 1181-1182.

Scheeres, D.J., and 15 colleagues, 2006. Extraordinary dynamical configuration of binary NEA 1999 KW4. Science, in press.

Shepard, M.K., and 12 colleagues, 2006. Radar and infrared observations of binary near-Earth Asteroid 2002 CE26. Icarus 184, 198-210.

Stanzel, R., 1978. Lightcurves and rotation period of minor planet 283 Emma. Astron. Astrophys. Suppl. Ser. 34, 373–376.

Storrs, A., Vilas, F., Landis, R., Wells, E., Woods, C., Zellner, B., Gaffey, M., 2001a. S/2001 (87) 1. IAU Circ. 7590.

Storrs, A., Vilas, F., Landis, R., Wells, E., Woods, C., Zellner, B., Gaffey, M., 2001b. S/2001 (107) 1. IAU Circ. 7599.

Tamblyn, P.M., Merline, W.J., Chapman, C.R., Nesvorný, D., Durda, D.D., Dumas, C., Storrs, A.D., Close, L.M., Menard, F., 2004. S/2004 (17246) 1. IAU Circ. 8293.

Taylor, P.A., Margot, J.-L., Nolan, M.C., Benner, L.A.M., Ostro, S.J., Giorgini, J.D., Magri, C., 2006. 2004 DC. CBET 535.

Tedesco, E.F., Noah, P.V., Noah, M., Price, S.D., 2002. The Supplemental IRAS Minor Planet Survey. Astron. J. 123, 1056-1085.

Torppa, J., Kaasalainen, M., Michałowski, T., Kwiatkowski, T., Kryszczyńska, A., Denchev, P., Kowalski, R., 2003. Shapes and rotational properties of thirty asteroids from photometric data. Icarus 164, 346-383.

Torppa, J., Virtanen, J., Muinonen, K., Laakso, T., Niemelä, J., Näränen, J., Aksnes, K. , Dai, Z., Lagerkvist, C-I., Rickman, H., Hahn, G., Michelsen, R., Grav, T., Jorgensen, U-G., 2006. Icarus, submitted.

Vokrouhlický, D., Nesvorný, D., Bottke, W.F. Jr., 2003. The vector alignments of asteroid spins by thermal torques. Nature 425, 147–151.

Walsh, K.J., Richardson, D.C., 2006. Binary near-Earth asteroid formation: Rubble pile model of tidal disruptions. Icarus 180, 201–216.

Walsh, K.J., Richardson, D.C., 2007. A steady-state model of NEA binaries formed by tidal disruption of gravitational aggregates. Icarus, submitted.

Warner, B.D., 2005. Asteroid lightcurve analysis at the Palmer Divide Observatory - winter 2004-2005. Minor Planet Bull. 32, 54-58.

Warner, B.D., Pravec, P., Pray, D., 2005a. (76818) 2000 $RG_{79}$. IAU Circ. 8592.

Warner, B.D., Pravec, P., Kušnirák, P., Cooney, W., Gross, J., Terrell, D., Nudds, S., 2005b. (3309) Brorfelde. CBET 279.

Warner, B.D., Pravec, P., Kušnirák, P., Cooney, W., Gross, J., Terrell, D., Higgins, D., Kornoš, L., Világi, J., Pray, D., Masi, G., Mallia, F., 2005c. (5477) 1989 $UH_2$. CBET 288.

Warner, B.D., Pray, D., Pravec, P., Cooney Jr., W., Gross, J., Terrell, D., 2005d. (34706) 2001 $OP_{83}$. CBET 341.

Warner, B.D., and 18 colleagues, 2005e. Binary Hungarias (5905) Johnson and (9069) Hovland, their relations to small binary Vestoids and NEAs. In: Asteroids, Comets, Meteors 2005, IAU Symp. 229, Abstract No. 10.14.

Warner, B.D., and 12 colleagues, 2006. Lightcurves analysis for Hungaria asteroids 3854 George, 4440 Tchantches and 4674 Pauling. Minor Planet Bull. 33, 34-35.